Morphological Contributions to Glass Transition in Poly(L-lactic acid)

Y. Wang,[†,‡] J. L. Gómez Ribelles,[§] M. Salmerón Sánchez,[§] and J. F. Mano*[,†,‡]

Polymer Engineering Department, University of Minho, Campus de Azurém, 4800-058 Guimarães, Portugal; 3B's Research Group—Biomaterials, Biodegradables and Biomimetics, University of Minho, Campus de Gualtar, 4710-057 Braga, Portugal; and Center for Biomaterials, Universidad Politécnica de Valencia, P.O. Box 22012, E-46071 Valencia, Spain

Received October 7, 2004; Revised Manuscript Received December 28, 2004

ABSTRACT: Poly(L-lactic acid) (PLLA) samples were prepared with different degrees of crystallinity, obtained during cooling from the melt at different scanning rates, and subjected to annealing below T_g. For intermediate crystallinities two endothermic peaks assigned to enthalpy recovery could be detected by differential scanning calorimetry (DSC) on heating, indicating the existence of two distinct glass transition dynamics. The morphology at different length scales was characterized using WAXS, SAXS, and polarized light microscopy to correlate the DSC results to the microstructure. The low-temperature process was assigned to the bulklike glass transition whereas the high-temperature one was attributed to the restricted motions of the amorphous phase confined by the crystalline structures. The position and broadness of the two endotherms were found to be essentially independent of the spherulitic content of the samples. This was related to the invariance of the lamellar morphology within a large range of degrees of crystallinity. The occurrence of the high-temperature process throughout such range allowed to attribute this process to the hindered motions of the mobile amorphous phase within the lamellar stacks.

Introduction

Poly(L-lactic acid), PLLA, is a very well-known biodegradable and biocompatible polyester, widely used in biomedical applications,[1−3] including wound closure, prosthetic implants, controlled drug delivery systems, and three-dimensional scaffolds for tissue engineering as well as in packaging and textile applications. A main feature of PLLA is its intrinsic low rate of crystallization,[4−6] being possible to produce polymer with different degrees of crystallinity. This parameter, and the general lamellar organization, may be controlled by adequate thermal histories[7] and will have an influence on properties such as mechanical performance as well as on its rate of hydrolytic or enzymatic degradability.[7−11]

In semicrystalline polymers the amorphous phase also influences intrinsically the mechanical properties, especially near the glass transition temperature.[12] Another important effect associated with the amorphous fraction of the polymer below T_g is the occurrence of structural relaxation: in the nonequilibrium glassy state the system tends slowly toward its thermodynamic equilibrium, and several physical and mechanical characteristics will change with time. As the glass transition temperature of PLLA ranges typically between 60 and 65 °C, we expect that upon implantation PLLA will exhibit time-dependent behavior due to this purely physical phenomenon, besides the effects associated with chain scission. Therefore, from a practical point of view, it is important to investigate structural relaxation, as well as the general glass transition behavior, on such systems. Some descriptive studies presented results on structural relaxation studied by differential scanning calorimetry (DSC) in PLLA or PDLLA.[13,14] A more quantitative analysis of structural relaxation and glass transition dynamics was reported more recently.[15] In that work DSC data were produced around T_g after different thermal histories in both quasi-amorphous and highly crystalline PLLA. The glass transition dynamics exhibited quite different characteristics in the two cases. For example, in the latter material the distribution of characteristic times for segmental mobility is broader and the glass transition is shifted to higher temperature, when compared with the quasi-amorphous one.[15] This is the result of a clear confinement effect due to the presence of the crystalline structure in semicrystalline polymers.

This problem can be included, from a fundamental point of view, among the general problem dealing with the behavior of materials that are geometrically confined on a nanometer spatial scale, such as 3D confinement (such as in nanoporous glasses or zeolites), 2D confinement (in silicate layers of nanocomposites or in layered block copolymers), or thin polymer films. The understanding of the finite-size effects on the materials' properties may be also relevant for technological reasons in areas such as chemical engineering, biomaterials, medicine, microelectronics, and a series of applications in nanotechnologies.[16−18]

Using different thermal histories in semicrystalline polymers, different lamellar structures may be produced. Therefore, this procedure allows to tailor, within a certain range, the nanometric confinement of the amorphous phase.[19,20] Therefore, semicrystalline systems may be also used as an adequate model for studying conformational mobility in confined geometries. Poly(ethylene therephthalate) (PET) has been widely used in this context. It would be interesting to extend such kinds of work to other semicrystalline polymeric systems, exhibiting different lamellar structures. Moreover, as will be discussed later, the origin of the confinement imposed by the crystalline environment is not fully understood. Is the dynamics of the amorphous phase changed between the lamellae or

† Polymer Engineering Department, University of Minho.
‡ 3B's Research Group, University of Minho.
§ Universidad Politécnica de Valencia.
* Author for correspondence: e-mail jmano@dep.minho.pt.

10.1021/ma047934i CCC: $30.25
Published on Web 05/04/2005

between the lamellar stacks regions? Do the glass transition features of the confined amorphous phase change with the total degree of crystallinity? A strategy to address such questions is to compare the glass transition behavior of both confined and bulklike amorphous phases with structural information, preferably in samples covering a broad range of degrees of crystallinity.

The influence of crystallinity on the dynamics of the amorphous phase in poly(lactic acid) has been carefully accessed by dielectric relaxation spectroscopy.[21,22] It was shown that this technique may provide quantitative information about the dynamic behavior of the polymeric chains throughout a wide frequency range. The rough experimental results could not discriminate, for intermediate degrees of crystallinity, the motions of both nonconfined and confined amorphous phases. Also for PET, for example, a continuous change of the position of the α-relaxation peak is observed in the frequency scale during isothermal crystallization, together with a broadening of the distribution of relaxation times.[23,24] More recently, some authors were able to deconvolute the overall dielectric glass transition signal into two α-relaxation processes using a fitting procedure.[25] However, it was shown that the glass transition of the two kinds of amorphous phases in PET could be clearly distinguished from experimentally DSC curves, looking at the endothermic peaks due to enthalpy recovery after a stage below T_g.[26−28] In this work a similar analysis will be performed in PLLA. Moreover, different degrees of crystallinity will be explored, and the morphology of the samples will be analyzed by both optical microscopy and X-ray scattering, which will assist in the attribution of the amorphous phase that is assigned to the observed glass transition processes.

Experimental Section

A Perkin-Elmer DSC7 was used to study the glass transition behavior of PLLA with different degrees of crystallinity and after an aging period below T_g, using nitrogen as a purge gas. Both temperature and heat flow were calibrated with indium. All the DSC experiments were carried out at 10 °C min^{-1} from 25 to 80 °C.

The PLLA used in this work is from Purac Biochem with molecular weights $\langle M_n \rangle = 86\,000$ and $\langle M_w \rangle = 151\,000$, evaluated from gel permeation chromatography (Shimadzu, LC 10A, Japan) using polystyrene as standard and chloroform as solvent. PLLA films of ∼0.2 mm thickness were obtained by hot pressing at about 200 °C and quenching them in cold water. Samples were cut from the films, with weights varying between 7 and 10 mg. Different crystallinities were introduced by melting samples in the DSC at 190 °C for 2 min, cooling at 200 °C min^{-1} to 160 °C, and then cooling at various rates, q^-, from 1 to 5 °C min^{-1}, down to room temperature. To erase the effect of the different cooling rates in the formation of glass phase, the samples were reheated to 78 °C and held for 5 min and then were quenched down to 45 °C and aged for 42 h in a tube furnace. After this aging period, the samples were quenched to room temperature and stored immediately in a refrigerator in order to freeze further structural relaxation before the DSC experiments.

For both wide-angle and small-angle X-ray scattering experiments, WAXS and SAXS, sample plates of ∼1 mm thickness were obtained by hot pressing at about 200 °C and quenching them in cold water. A Mettler hot-stage (FP80) was used to obtain different crystallinities, following the same procedures of thermal treatment as that for DSC experiments. The same samples were also used for polarized optical microscopy (Olympus BH-2 optical microscope). Thin films of 10 μm were cut from the plates using a microtome (Leitz 1401) and then embedded in epoxy resin between microscope glass slides under a certain load for 1 day. WAXS and SAXS experiments were performed using X-ray synchrotron radiation (transmission mode) at the Soft Condensed Matter A2 beamline at HASYLAB (DESY) synchrotron facility in Hamburg (Germany). The experimental setup includes a MARCCD detector for acquiring two-dimensional SAXS patterns (sample-to-detector distance being 280 cm) and a linear detector for 1-D WAXS measurements (distance 23 cm). Cu Kα radiation, with a wavelength of $\lambda = 0.154$ nm, was employed for both SAXS and WAXS measurements.

Results and Discussion

The DSC thermograms recorded on heating of all samples after the aging period (42 h at 45 °C) are shown in Figure 1 (solid lines). For each sample the first heating ended at 80 °C, followed by a quenching down to 25 °C, after which a second heating has performed (dashed line). The interpretation of the results taken from the quenched samples (second runs) is difficult, especially for the samples previously subjected to a slow cooling from the melt where the glass transition was barely detectable. Moreover, for intermediate cooling rates, it is hard to resolve eventual different glass transition processes in such curves. However, the previous aging process noticeably enhances the molecular processes involved in the glass transition of the materials (first runs). For q^- of 1 and 1.5 °C min^{-1}, an endothermic peak is found at 70.2 and 67.5 °C, respectively. For the highest q^- (4 and 5 °C min^{-1}) basically a narrow peak is observed around 64 °C. The nature of these two peaks is different, as analyzed in detail before, by treating DSC data obtained on both amorphous and semicrystalline PLLA after subjected to different thermal histories below T_g, using a phenomenological model based on configurational entropy.[15] It was found in that work that the exponent β of the KWW equation is lower for the semicrystalline material than for the amorphous one, indicating a difference in the distribution of relaxation times; the same conclusion was achieved in PET.[26] However, the study in ref 15 was only carried out in the two extremes of crystallinity content. A question that could be raised here is how these two dynamics would progress with the degree of crystallinity from a material almost amorphous toward a highly semicrystalline one. Figure 1 shows that for intermediate q^- the curves display two endothermic peaks. A similar behavior was found in PET, although in a restricted number of degrees of crystallinity.[26−28] During the aging period below T_g the mobile polymeric segments will relax toward equilibrium. During heating the recovery of the enthalpy will happen at temperatures that will depend on the mobility of the chains. The lower temperature peak in Figure 1 corresponds to the glass transition dynamics of a less-hindered amorphous phase, similar to the bulk one. In fact, for a sample quenched from the melt, with no spherulitic content, only the low-temperature peak was observed, at the same temperature position and with similar shape (not shown). The higher temperature peak arises from the mobility of a confined amorphous phase, such as the one appearing in the more crystalline material ($q^- = 1$ °C min^{-1}).

An important finding is that during the evolution of q^- the positions of the two peaks are maintained approximately at the same position: for q^- from 2 to 3.5 °C min^{-1} the higher temperature peak (higher T_g process) has a maximum at 69 ± 1 °C, and the lower temperature one is found at 65 ± 0.5 °C. This provides

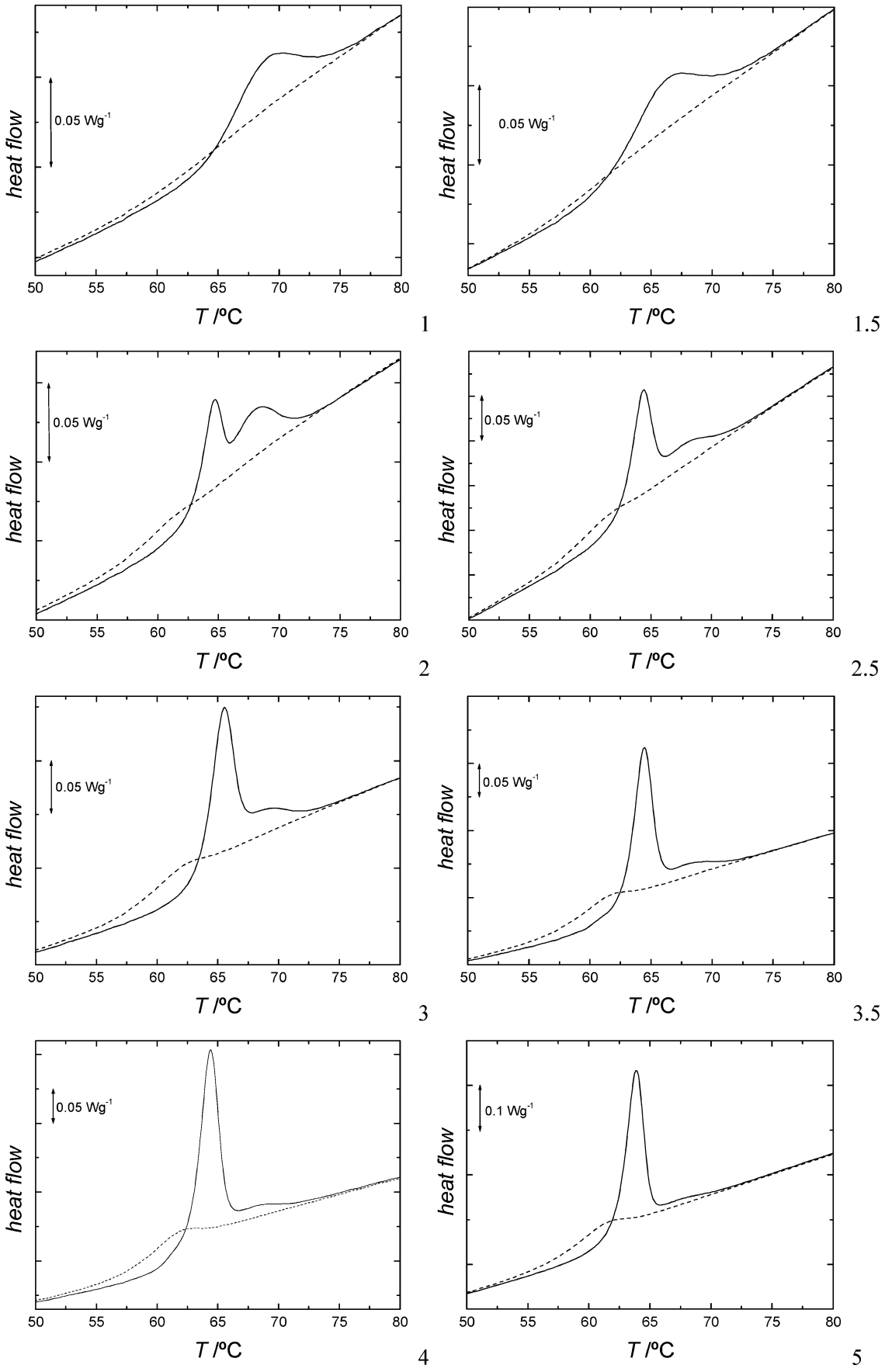

Figure 1. DSC scans obtained at 10 °C min^{-1}, from 25 to 80 °C, on the PLLA samples prepared by cooling from the melt at different rates, q^- (indicated in the graphics in °C min^{-1}). Solid lines: first heating thermograms obtained after an aging period at 45 °C for 42 h. Dashed lines: second scan obtained by immediately quenching the sample from 80 °C down to 25 °C after the first run.

a clear indication that the system shows two distinct glass transition dynamics that exhibit quite independent behaviors and that do not depend significantly on the crystallinity content.

The evolution of segmental dynamics in PLLA with crystallinity was also previously followed by dielectric relaxation spectroscopy. During crystallization of PLLA, from both melt and glass, Mijovic and Sy[21] detected, as expected, a continuous decrease of the intensity of the dielectric loss peak of the α-relaxation during crystallinity development; surprisingly, the position of the peak in the frequency axis did not vary upon crystallization. However, another study clearly showed a slowing down of the segmental dynamics with increasing crystallinity in PLLA[22] and explained the data reported in ref 21 as a result of an insufficient crystallinity level reached by the system.

First, it would be helpful to discuss the effect of a general confinement due to the existence of a crystalline fraction surrounding amorphous regions. As found in most polymers, this effect is associated with an increase of T_g.[29] It is to be noticed that this may not be the general case for other sorts of confinements. For example, poly(propylene glycol) confined in silica-based nanoporous glasses exhibited lower T_gs with respect with the bulk material when pore sizes are 5, 7.5, and 20 nm;[30] however, for pore sizes of 2.5 nm an increase of T_g is found. Such a diversity of behaviors, resumed for example in ref 29, has been attributed by some authors to a competition between two different contributions.[30−32] First, there is the effect of the geometrical confinement itself, where the length scale associated with conformation mobility, in the framework of the Adam and Gibbs theory,[33] increases with decreasing temperature being limited by the size of the confinement if it is of the order of a few nanometers (i.e., close to the length scale of the material's molecular fluctuations at T_g); according to these authors, this gives rise to an acceleration of the molecular mobility, leading to a reduction of T_g with respect to the bulk. An opposite effect results from the influence of the surface interaction with the relaxing entities: attractive interactions between the mobile and surface molecules results in a slowing down of the relaxation times and hence to an increase of T_g. Similar effects were found in low molecular weight glass-formers as propylene glycol.[34,35] Taking into account this picture, we may conclude that this later "adsorption" effect is dominant in the confinement induced by the crystalline phase in semicrystalline polymers. In such systems one should have thus a favorable interaction between the mobile amorphous phase and molecular groups of the confinement scaffold in contact with it, which would be constituted by the so-called rigid amorphous phase.[36] A major reason could be related to the fact that there are polymeric chains in the interface region sharing both mobile and rigid regions, enhancing thus the interaction between the phases. We will assume that the extent of the confinement for a particular system, that will be reflected, for example, by the increase of T_g, will be mainly determined by the thickness of the mobile amorphous phase region. However, we should analyze further what this amorphous phase should be.

It would be helpful in this context to get further information about the morphology at different length scales of the PLLAs studied. This can be informative to elucidate on the relationship between structure and the two different dynamics observed for conformational mobility. Optical micrographs of the samples obtained at different cooling rates are shown in Figure 2. Similar pictures were shown by Mijovic and Sy, obtained during isothermal crystallization.[21] The results clearly demonstrate that the studied samples exhibited a wide range of spherulitic content and thus a great variety of degrees of crystallinity.

Further analysis was carried out by WAXS where one-dimensional scattering profiles are shown in Figure 3. The calculation of the degree of crystallinity, X_c, was performed by treating each WAXS pattern according to the method used in ref 37: two Gaussian peaks riding on a baseline were used to fit the amorphous background, and the ensemble of the crystalline diffraction peaks was described by 6 Gaussian curves; X_c was calculated by dividing the total intensity of the crystalline reflections with the overall intensity. Values of X_c ranging between 7 and 46% were obtained for the different q^-. In Figure 4 this parameter is plotted against the amount of the area occupied by the spherulites in the polarized microscopy data, obtained by treating the pictures in Figure 2 with an image analyzer software. This figure shows a fairly good correlation between the amount of spherulites and the crystallinity between q^- from 1 to 3 °C min^{-1}, which suggests that the overall degree of crystallinity is mainly controlled by the amount of spherulites. Moreover, the inset of Figure 3 shows that the half-width (in radians) of the two major diffraction peaks, β, does not change systematically with q^-. This would indicate that the PLLA apparent lateral crystal sizes, L_{hkl}, do not depend significantly on q^-, as L_{hkl} is intimately related to β by Scherrer's equation:[38] $L_{hkl} = k\lambda/(\beta \cos \theta)$, where k is a constant, being about 0.9 for most polymeric systems, and λ is the wavelength of radiation used. This may be an indication that the crystalline fraction and crystalline dimensions within the spherulites weakly depend on the cooling rate, at least for $q^- < 3$ °C min^{-1}. Therefore, the total degree of crystallinity is mainly determined by the content of spherulites in the volume.

More insight at the nanoscale level may be achieved by SAXS. Figure 5 shows SAXS patterns of the different samples analyzed as a function of the scattering vector, $s = (2/\lambda) \sin(\theta/2)$. The long spacing was calculated by $L = 1/s_{max}$, s_{max} being the scattering vector of maximum intensity of the Lorentz-corrected SAXS curves. For q^- higher than 2.5 °C min^{-1} the amount of spherulites was too small to resolve the lamellar structure from SAXS. Moreover, the differences in the densities of the amorphous and crystalline phases in PLLA are small, which renders particularly difficult to collect SAXS patterns in this system. For q^- of 1.5, 2, and 3 °C min^{-1}, where more drastic changes are observed in the DSC data, the long period is similar (L between 20 and 21 nm). Such values are typical for PLLA (e.g., ref 39). The fraction of mobile amorphous phase, X_{maf}, in PLLA crystallized at different temperatures was shown to vary between 18 and 27%.[22] Therefore, assuming a simple two-phase microstructure, consisting of continuous lamellar stacks, as well as a similar density for both amorphous and crystalline phases, we could estimate, from the product of L and X_{maf}, that the mobile amorphous layers would have average thicknesses in the range of 3.6 and 5.7 nm.

As proposed by other authors,[19,20] this mobile amorphous layer confined between crystalline lamellae should be on the origin of the slow glass transition dynamics

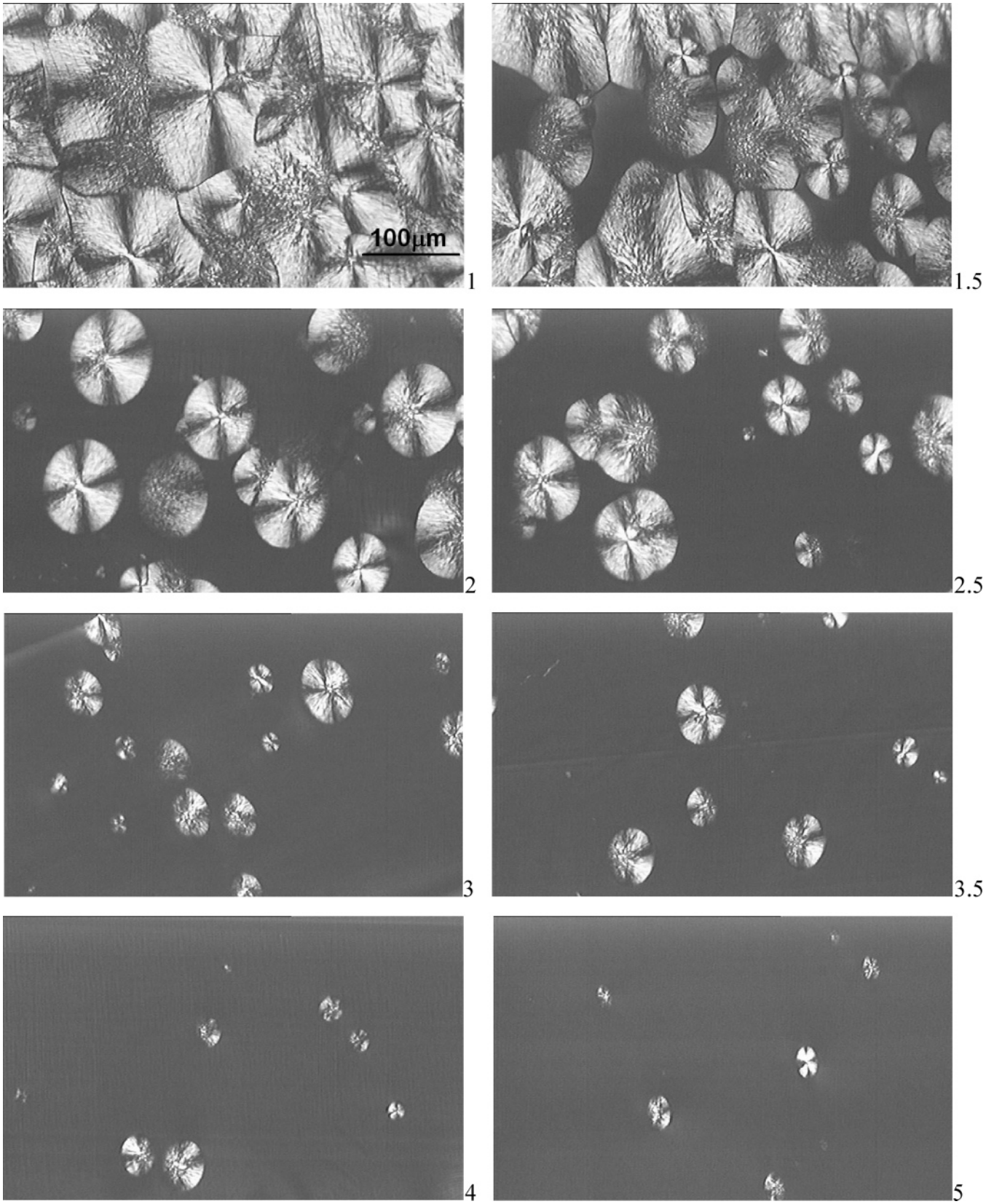

Figure 2. Representative polarized optical micrographs obtained at room temperature for the PLLA samples prepared after different q^- (the same as in Figure 1).

detected in semicrystalline polymers. Therefore, the temperature difference between the two structural relaxation peaks observed by DSC are expected to be dependent on the thickness of the interlamellar mobile amorphous phase. For PET such differences are close to 10 °C,[28] whereas for PLLA we found 4 °C. This may reflect the higher confinement of the amorphous phase, as the thickness of the free amorphous phase between the lamellae in PET is typically below 3.2 nm.[20]

However, another interesting hypothesis has been proposed for the source of the amorphous phase that gives rise to the slower process,[25] based on simultaneous

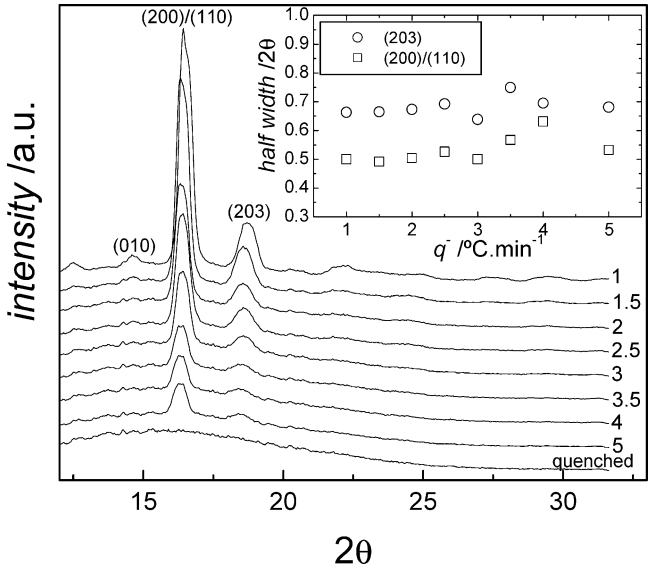

Figure 3. Wide-angle X-ray scattering patterns for the PLLA samples crystallized upon different cooling rates, q^- (indicated next to the curves, in °C min^{-1}). The half-width of the two main diffraction peaks, corresponding to the (200)/(110) and (203) diffraction planes, are shown in the inset graphics as a function of q^-.

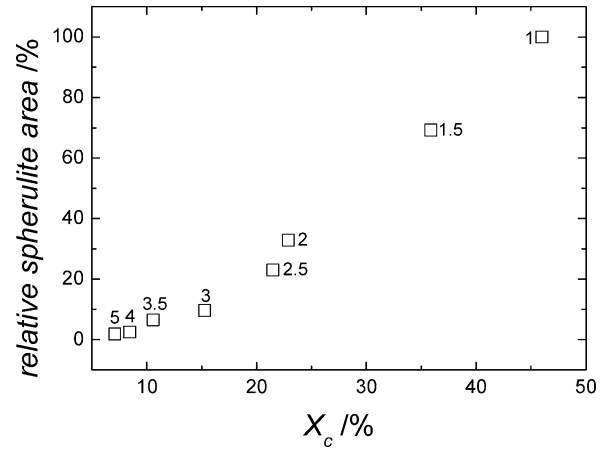

Figure 4. Area ratio occupied by spherulites in the optical microscopy pictures (data taken from Figure 2) as a function of the overall crystallinity degree (obtained from the WAXS data), for the samples obtained at the different q^- (indicated next to the experimental points, at °C min^{-1}).

dielectric relaxation spectroscopy and X-ray scattering measurements in PET. It is suggested that the interlamellar amorphous phase is rigid and does not participate in any α-relaxation. During primary crystallization lamellar stacks are formed, even in the early stages,[40] where (i) the interlamellar amorphous phase is dynamically arrested and (ii) the amorphous phase between the lamellar stacks (intralamellar stacks amorphous phase) is as mobile as the bulk one as long as the lamellar stacks are well separated from each other.[25] Therefore, during this first process we should only observe a reduction of the intensity of the glass transition process as a result of the formation of the primarily lamellae, without any change in the dynamics. Upon secondary crystallization secondary lamellar stacks starts to develop within the liquid pockets existing between primary lamellar stacks.[41,42] The hindered dynamic process is assigned to the segmental mobility of the amorphous chains that will be confined in this liquid pockets in which secondary lamellae started to

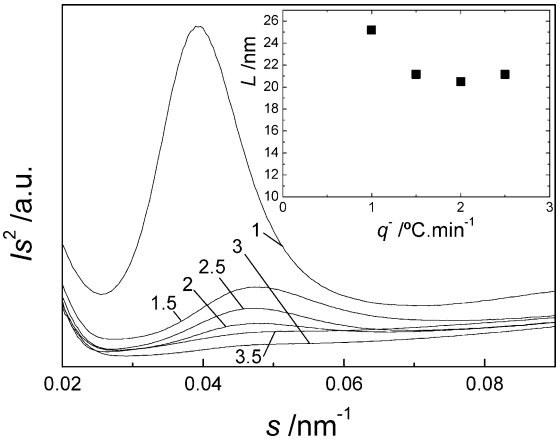

Figure 5. Lorentz-corrected small-angle X-ray scattering patterns for PLLA samples crystallized at different cooling rates from 1 to 3.5 °C min^{-1} (indicated next to each curve). The inset graphics shows the variation of the long period, L, with q^-.

grow, which should occur in later stages of crystallization.[25] After deconvoluting the main dielectric peak, Alvarez et al. found that the slower process appear only beyond a given crystallinity level that should correspond to the onset of secondary crystallization.

In the particular case of the system studied in the present work, both processes appear simultaneously and independently whenever spherulites and interspherulitic regions are both present, i.e., throughout a very large range of degrees of crystallinity. This includes the presence of a confined glassy phase at the early crystallization stages that gives rises to the higher T_g process, where presumably secondary crystallization had not yet occurred, with similar characteristics of the confined glassy phase present in a much extended crystallization stage. Moreover, we may conclude, from a qualitative comparison of Figures 1 and 2, that the evolution of the relative magnitude of the two DSC peaks follows approximately the spherulitic development, and from the results of Figure 4, it also follows the overall degree of crystallinity: as the amount of crystalline phase increases, we observe a progressive intensity enhancement of the hindered glass transition process and a depletion of the bulklike mechanism. Moreover, both processes maintain their main characteristics, namely their shape and temperature position.

From the above observations, we suggest, at least for the case of the system studied in this work, that the low-temperature glass transition is assigned to the segmental motions within interspherulitic amorphous phase. The high-temperature process should be assigned to the presence of intraspherulitic amorphous phase, probably confined within the primary (or secondary) lamellar stacks.

Main Conclusions

PLLA samples can be obtained with a wide range of degrees of crystallinity, exhibiting a clearly defined spherulitic structure, by cooling the melt at different rates down to room temperature. This provides an adequate model to systematically study the influence of crystallinity on the glass transition dynamics. After subjecting these samples to an aging process below T_g, two well-distinguished endothermic peaks can be found when both intraspherulitic and interspherulitic amorphous phases are present, corresponding to the glass

transition of a bulklike process (at lower temperatures) and a broad process assigned to the glass transition of a confined mobile amorphous phase. The position in the temperature axis and the general shape of these peaks do no change significantly with the degree of crystallinity. The effect of confinement exerted by crystalline phase should be mainly dominated by the nature of the interface between the free amorphous phase and the rigid phase (adsorption effect) and not due to the geometrical confinement itself. In fact, according to previous works, the geometrical confinement effect should lead to a decrease of T_g in the confined phase and the opposite behavior is found in typical semicrystalline systems. As the higher temperature glass transition process is present even in the early stages of crystallization, we assigned it to the molecular motions of the interlamellar amorphous phase. Such kinds of systematic work should be extended in other semicrystalline systems in order to check any universal behavior on the effect of crystalline confinement in polymers.

Acknowledgment. Y.W. and J.F.M. acknowledge the financial support provided by FCT through the POCTI and FEDER programs. Y.W. thanks the PostDoc Grant from Portuguese Foundation for Science and Technology (SFRH/BPD/11497/2002). M.S.S. and J.L.G.R. acknowledge the support of the Spanish Science and Technology Ministry through the MAT2001-2678-C02-01 project. The authors also thank Dr. Z. Denchev for useful discussions concerning the X-ray scattering data.

References and Notes

(1) Södegard, A.; Stolt, M. *Prog. Polym. Sci.* **2002**, *27*, 1123−1163.
(2) Thomson, R. C.; Wake, M. C.; Yaszemski, M. J.; Mikos, A. G. *Adv. Polym. Sci.* **1995**, *122*, 245.
(3) Kim, H. D.; Bae, E. H.; Kwon, I. C.; Pal, R. R.; Nam, J. D.; Lee, D. S. *Biomaterials* **2004**, *25*, 2319.
(4) Iannace, S.; Nicolais, L. *J. Appl. Polym. Sci.* **1997**, *64*, 911.
(5) Miyata, T.; Masuko, T. *Polymer* **1998**, *39*, 5515.
(6) Di Lorenzo, M. L. *Polymer* **2001**, *42*, 9441.
(7) Tsujo, H.; Ikada, Y. *Polymer* **1995**, *36*, 2709.
(8) Reeve, M.; McCarthy, S.; Downey, M.; Gross, R. *Macromolecules* **1994**, *27*, 825.
(9) Cam, D.; Hyon, S.; Ikada, Y. *Biomaterials* **1995**, *16*, 833.
(10) MacDonald, R.; McCarthy, S.; Gross, R. *Macromolecules* **1996**, *29*, 7356.
(11) Tsuji, H.; Ikada, Y. *Polym. Degrad. Stab.* **2000**, *67*, 179.
(12) Loo, L. S.; Cohen, R. E.; Gleason, K. K. *Science* **2000**, *288*, 116.
(13) Celli, A.; Scandola, M. *Polymer* **1992**, *33*, 2699.
(14) Liao, K.; Quan, D.; Lu, Z. *Eur. Polym. J.* **2002**, *38*, 157.
(15) Mano, J. F.; Gómez Ribelles, J. L.; Alves, N. M.; Salmerón Sanchez, M., submitted for publication.
(16) Drake, J. M., Grest, G. S., Klafter, J., Kopelman, R., Eds.; Dynamics in small confining systems IV. *Mater. Res. Soc. Symp. Proc.* **1998**, *543*.
(17) Frick, B., Zorn, R., Buttner, H., Eds.; 1st international workshop on dynamics in confinement. *J. Phys. IV* **2000**, *10*, *Pr7*.
(18) Frick, B.; Koza, M.; Zorn, R. 2nd international workshop on dynamics in confinement. *Eur. Phys. J. E* **2003**, *12*.
(19) Schick, C.; Donth, E. *Phys. Scr.* **1991**, *43*, 423.
(20) Dobbertin, J.; Hensel, A.; Schick, C. *J. Therm. Anal.* **1996**, *47*, 1027.
(21) Mijovic, J.; Sy, J.-W. *Macromolecules* **2002**, *35*, 6370.
(22) Kanchanasopa, M.; Runt, J. *Macromolecules* **2004**, *37*, 863.
(23) Ezquerra, T. A.; Baltà-Calleja, F. J.; Zachmann, H. G. *Polymer* **1994**, *35*, 2600.
(24) Fukao, K.; Miyamoto, Y. *J. Non-Cryst. Solids* **1997**, *212*, 208.
(25) Alvarez, C.; Šics, I.; Nogales, A.; Denchev, Z.; Funari, S. S.; Ezquerra, T. A. *Polymer* **2004**, *45*, 3953.
(26) Alves, N. M.; Mano, J. F.; Balaguer, E.; Meseguer Dueñas, J. M.; Gómez Ribelles, J. L. *Polymer* **2002**, *43*, 4111.
(27) Montserrat, S.; Cortés, P. *J. Mater. Sci.* **1995**, *30*, 1790.
(28) Zhao, J.; Song, R.; Zhang, Z.; Linghu, X.; Zheng, Z.; Fan, Q. *Macromolecules* **2001**, *34*, 343.
(29) McKenna, G. B. *J. Phys. IV* **2000**, *10*, *Pr7*, 53.
(30) Schönhals, A.; Goering, H.; Brzezinka, K. W.; Schick, C. *J. Phys.: Condens. Matter* **2003**, *15*, S1139.
(31) Kremer, F.; Hartmann, L.; Serghei, A.; Pouret, P.; Léger, L. *Eur. Phys. J. E* **2003**, *12*, 139.
(32) Schönhals, A.; Goering, H.; Schick, C.; Frick, B.; Zorn, R. *Colloid Polym. Sci.* **2004**, *282*, 882.
(33) Adam, G.; Gibbs, J. H. *J. Chem. Phys.* **1965**, *43*, 139.
(34) Pissis, P.; Kyritsis, A.; Daoukaki, D.; Barut, G.; Pelster, R.; Nimtz, G. *J. Phys.: Condens. Matter* **1998**, *10*, 6205.
(35) Barut, G.; Pissis, P.; Pelster, R.; Nimtz, G. *Phys. Rev. Lett.* **1998**, *80*, 3543.
(36) Cheng, S. Z. D.; Zu, Z. Q.; Wunderlich, B. *Macromolecules* **1987**, *20*, 2802.
(37) Mano, J. F.; Wang, Y.; Viana, J. C.; Denchev, Z.; Oliveira, M. J. *Macromol. Mater. Eng.* **2004**, *289*, 910.
(38) Alexander, L. E., Ed.; *X-ray Diffraction Methods in Polymer Science*; Wiley-Interscience: New York, 1969; p 137.
(39) Park, J. W.; Im, S. S. *J. Polym. Sci., Polym. Ed.* **2002**, *40*, 1931.
(40) Lin, L.; Chan, C.-M.; Yeung, K. L.; Li, J.-X.; Ng, K.-M.; Lei, Y. *Macromolecules* **2001**, *34*, 316.
(41) Verma, R.; Marand, H.; Hsiao, B. *Macromolecules* **1996**, *29*, 7767.
(42) Wang, Z. G.; Hsiao, B. S.; Sauer, B. B.; Kampter, W. G. *Polymer* **1999**, *40*, 4615.

MA047934I